

Linear Colour-Dependent Image Filtering based on Vector Decomposition

Stephen J. Sangwine & Barnabas N. Gatszeni
University of Essex

Department of Electronic Systems Engineering
Wivenhoe Park, Colchester, CO4 3SQ, UK

Email: s.sangwine@ieee.org, bgatsh@essex.ac.uk

Todd A. Ell

5620 Oak View Court,
Savage, Minnesota, USA

Email: t.ell@ieee.org

ABSTRACT

This paper presents a new method for devising linear colour-dependent filters based on decomposition of an image into components parallel and perpendicular to a chosen direction in colour space. The components may be separately filtered with linear filters and added to produce an overall result. The paper demonstrates this approach with a colour-selective averager, and then shows that the filter may be implemented without the parallel/perpendicular decomposition by adding the output of two filters, derived in the paper. The approach is based on quaternion algebra and convolution.

1 Introduction

Linear filtering of colour images is a very recent development. The first linear colour filter was published by Sangwine [1] and was a colour edge detector based on convolution with hypercomplex masks. Two years later, Evans, Sangwine and Ell published two papers [2, 3], again based on hypercomplex convolution, but this time providing colour-sensitive smoothing or edge detection. The approach taken in these two papers was somewhat *ad-hoc* and did not suggest a more general approach. In this paper, we present a general approach to colour-sensitive linear filtering, and for the first time we show how a hypercomplex linear vector filter may be derived from first principles.

The work presented here is part of a larger project to study hypercomplex filtering of colour images. The particular filter presented in this paper is a very simple colour-selective averager, but the principle demonstrated is likely to lead to more sophisticated filters. Throughout this paper, colour image pixels are represented by hypercomplex numbers (quaternions). The quaternion mathematical relations relevant to the work contained in this paper are included in Appendix A.

Our aim in the work presented in this paper is to develop methods for the design of colour-sensitive linear vector filters applicable to colour images. Our approach is based on quaternion algebra and convolution with quaternion-valued (or hypercomplex) masks and composition of a linear vector filter from linear operations, in classic fashion. Convolution with a quaternion-valued mask is a linear operation, and so is the decomposition of an image into images with pixels parallel and perpendicular to a chosen direction in colour space.

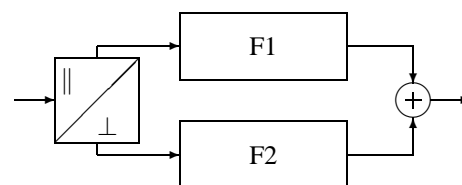


Figure 1: Filtering with two linear filters F1 and F2 operating on separated parallel and perpendicular image components.

2 The Colour-Selective Filter

A colour-selective filter may be implemented by first decomposing the image into components parallel to and perpendicular to a chosen direction in colour space. For example, to make a filter sensitive to cyan, we could decompose the image pixel-by-pixel into an image with pixels parallel to the cyan direction, and an image with pixels perpendicular to the cyan direction. These two images, if added pixel-by-pixel, will reconstruct the original image. This decomposition is exactly equivalent to resolving the pixel vectors into the chosen direction, and subtracting the resolved vectors from the original pixels.

Once we have separated the image into two components, parallel to and perpendicular to the chosen colour direction, we are free to filter either or both of the separated images. Provided the filtering is linear, we may then recombine the filtered separated images to produce a result. The process is shown diagrammatically in Figure 1.

Our objective, not so far realised, is to combine all these steps into *one* hypercomplex convolution as shown in Figure 2.

The scheme in Figure 3 was achieved through studying a particular case where F1 in Figure 1 is a scalar averager and F2 is an all-pass filter, as shown in Figure 4. For this particular case we have obtained equivalent filters F3 and F4 as shown in Figure 3, thus merging the parallel/perpendicular decomposition step into the convolutions. It turns out that one of the convolutions is a scalar convolution, and the other requires a quaternion convolution, but this may not be general. In the next section we present the algebraic derivation of the F3 and F4 filters.

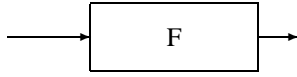


Figure 2: This is a single filter which must perform the same function as the filters in Figure 1 and Figure 3.

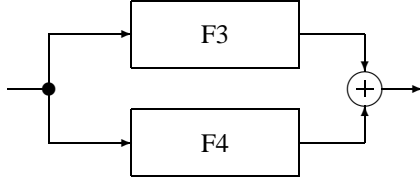


Figure 3: Filtering with no decomposition of the image into parallel and perpendicular components.

3 An example Filter

The parallel ν_{\parallel} and perpendicular component ν_{\perp} of each pixel is given by [4]:

$$\nu_{\parallel} = \frac{1}{2}(\nu - \mu\nu\mu), \quad \nu_{\perp} = \frac{1}{2}(\nu + \mu\nu\mu) \quad (1)$$

where μ and ν represent the axis for the chosen colour direction and the pixel value respectively.

Only the parallel component in Figure 4 was filtered using a 5×5 averager with mask coefficients of $\frac{1}{25}$. The (1×1) all-pass filter had a single equivalent coefficient with a value of 1.

The coefficients from a 5×5 mask were combined with the expressions given in (1) to obtain the equations shown in Table 1. These equations were then implemented as part of the convolutions F3 and F4 in Figure 3 where the perpendicular/parallel separation has been eliminated.

$$\frac{1}{50}(\nu - \mu\nu\mu) + \frac{1}{2}(\nu + \mu\nu\mu) = \frac{13}{25}\nu + \frac{2\mu\sqrt{3}}{5}\nu - \frac{2\mu\sqrt{3}}{5} \quad (2)$$

Simplifying the expression of the central pixel in Table 1 gives (2). The second term in (2) on the RHS is a pure quaternion.

The relations (1) and (2) and in Table 1 will be used in this discussion. Since $N = 5$ from using the 5×5 mask for the averager, on LHS of (2) the ν_{\parallel} is multiplied by $\frac{1}{N^2}$ and hence its coefficients are altered. In the case of an all-pass filter, $N = 1$ thus the relation for ν_{\perp} in (2) is unaltered.

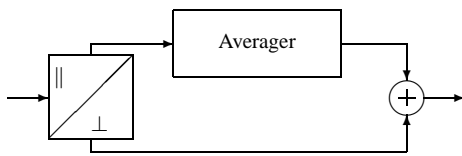


Figure 4: Colour-sensitive averaging filter.

$-\frac{1}{50}$	$-\frac{1}{50}$	$-\frac{1}{50}$	$-\frac{1}{50}$	$-\frac{1}{50}$
$-\frac{1}{50}$	$-\frac{1}{50}$	$-\frac{1}{50}$	$-\frac{1}{50}$	$-\frac{1}{50}$
$-\frac{1}{50}$	$-\frac{1}{50}$	$\frac{13}{25}$	$-\frac{1}{50}$	$-\frac{1}{50}$
$-\frac{1}{50}$	$-\frac{1}{50}$	$-\frac{1}{50}$	$-\frac{1}{50}$	$-\frac{1}{50}$
$-\frac{1}{50}$	$-\frac{1}{50}$	$-\frac{1}{50}$	$-\frac{1}{50}$	$-\frac{1}{50}$

Table 2: F3 mask.

$\frac{1}{5\sqrt{2}}\mu$	$\frac{1}{5\sqrt{2}}\mu$	$\frac{1}{5\sqrt{2}}\mu$	$\frac{1}{5\sqrt{2}}\mu$	$\frac{1}{5\sqrt{2}}\mu$
$\frac{1}{5\sqrt{2}}\mu$	$\frac{1}{5\sqrt{2}}\mu$	$\frac{1}{5\sqrt{2}}\mu$	$\frac{1}{5\sqrt{2}}\mu$	$\frac{1}{5\sqrt{2}}\mu$
$\frac{1}{5\sqrt{2}}\mu$	$\frac{1}{5\sqrt{2}}\mu$	$\frac{2\sqrt{3}}{5}\mu$	$\frac{1}{5\sqrt{2}}\mu$	$\frac{1}{5\sqrt{2}}\mu$
$\frac{1}{5\sqrt{2}}\mu$	$\frac{1}{5\sqrt{2}}\mu$	$\frac{1}{5\sqrt{2}}\mu$	$\frac{1}{5\sqrt{2}}\mu$	$\frac{1}{5\sqrt{2}}\mu$
$\frac{1}{5\sqrt{2}}\mu$	$\frac{1}{5\sqrt{2}}\mu$	$\frac{1}{5\sqrt{2}}\mu$	$\frac{1}{5\sqrt{2}}\mu$	$\frac{1}{5\sqrt{2}}\mu$

Table 3: F4: is a left mask (The right mask has identical values negated)

The centre and outer pixel values for F3 in Figure 3 are $\frac{13}{25}$ and $\frac{1}{50}$ respectively whereas for F4 they are $\frac{2\sqrt{3}}{5}[\]\frac{2\sqrt{3}}{5}\mu$ and $\frac{1}{5\sqrt{2}}[\]\frac{1}{5\sqrt{2}}\mu$ respectively. The respective masks are shown as Table 3 and Table 2. Table 3 is the left quaternion (its conjugate gives the right mask) mask.

4 Experimental results

We have sampled the tulips image shown in Figure 5 to obtain colours corresponding to the red of the petals, the green of the leaves and the yellow inside the flower. The RGB values were recorded as shown in Table 4. For a 24-bit colour image the origin has coordinates (127.5, 127.5, 127.5). Thus the colour component values have been reduced by 127.5 in order to conform to the RGB colour space as illustrated in Table 5. We use offset 8-bit RGB space in which (0,0,0) represents mid-grey. The image was decomposed into compo-

		RGB values		
		R	G	B
colours	green leaves	60	125	125
	red petals	225	90	90
	yellow	230	210	0

Table 4: RGB values read from tulips image

nents parallel and perpendicular to a chosen colour direction (axis μ). The 5×5 averager with entries of $\frac{1}{N^2}$ was used for filtering the image in the parallel direction. N is the size of the mask. This procedure is also illustrated by Figure 4.

The procedure for performing this filtering was as follows:

- convert pixel values to offset RGB space.
- select a colour (μ).
- split the image into the perpendicular and parallel components (specify the colour direction for the decomposition).

$\frac{1}{50}(\nu - \mu\nu\mu)$	$\frac{1}{50}(\nu - \mu\nu\mu)$	$\frac{1}{50}(\nu - \mu\nu\mu)$	$\frac{1}{50}(\nu - \mu\nu\mu)$	$\frac{1}{50}(\nu - \mu\nu\mu)$
$\frac{1}{50}(\nu - \mu\nu\mu)$	$\frac{1}{50}(\nu - \mu\nu\mu)$	$\frac{1}{50}(\nu - \mu\nu\mu)$	$\frac{1}{50}(\nu - \mu\nu\mu)$	$\frac{1}{50}(\nu - \mu\nu\mu)$
$\frac{1}{50}(\nu - \mu\nu\mu)$	$\frac{1}{50}(\nu - \mu\nu\mu)$	$\frac{1}{50}(\nu - \mu\nu\mu) + \frac{1}{2}(\nu + \mu\nu\mu)$	$\frac{1}{50}(\nu - \mu\nu\mu)$	$\frac{1}{50}(\nu - \mu\nu\mu)$
$\frac{1}{50}(\nu - \mu\nu\mu)$	$\frac{1}{50}(\nu - \mu\nu\mu)$	$\frac{1}{50}(\nu - \mu\nu\mu)$	$\frac{1}{50}(\nu - \mu\nu\mu)$	$\frac{1}{50}(\nu - \mu\nu\mu)$
$\frac{1}{50}(\nu - \mu\nu\mu)$	$\frac{1}{50}(\nu - \mu\nu\mu)$	$\frac{1}{50}(\nu - \mu\nu\mu)$	$\frac{1}{50}(\nu - \mu\nu\mu)$	$\frac{1}{50}(\nu - \mu\nu\mu)$

Table 1: 5×5 colour-sensitive averaging filter mask

		RGB values		
		R	G	B
colours	green leaves	-67.5	-2.5	-2.5
	red petals	97.5	-37.5	-37.5
	yellow	102.5	82.5	-127.5

Table 5: The values after subtracting 127.5 from each value in Table 4



Figure 5: Original tulips image

- average the parallel component.
- combine the filtered parallel component with the unfiltered perpendicular component.
- add offset, to obtain normal RGB image.

The results from this experiment (splitting, filtering and recombining) are shown in Figure 6.

- for the red petals direction, the observed colour is a blurred red colour on the red petal edges
- for the green direction, the result is a blurred green colour on the leaves
- for the yellow direction, the result is a blurred yellow colour on the yellow inside of the flower.

The results from the “difference images” are shown on the bottom row in Figure 6 were as follows: In the red colour direction, colours observed were cyan and red, in the yellow colour direction the colours observed were yellow and magenta and on the green colour direction, the colour observed was red. It can be noted that each result gives that particular colour and its opponent colour and thus they conform to the RGB colour space representation.

These results are dependent on the order of the difference. Here the filtered image was subtracted from the original image, otherwise if the original image had been subtracted from the filtered version, then the non-zero areas should have been identical to the filter axis rather than opponent colours.

The filtering of a parallel component of a quaternion image decomposed into two orthogonal components has been successfully accomplished.

We have done the equivalent filtering with the scheme of Figure 3 and obtained identical results, thus verifying the mathematics in (1) and (2). The scheme of Figure 3 is simple to implement as it requires no decomposition step.

5 Conclusion

Colour image filtering applied to one of the two orthogonal components obtained from the decomposition of a quaternion image has been developed. Good results were obtained for each colour direction filtered. As a consequence, a range of colours defined in the colour space by their vectors can be filtered. In terms of further work, replacing 2 filters discussed above by just a single filter is attractive. The filter of Figure 3 is a quaternion algebraic convolution without the need for parallel/perpendicular decomposition. This is a significant step in linear vector filtering of colour images.

Acknowledgements

The work of Barnabas N. Gatsheni was funded by the UK Engineering and Physical Sciences Research Council under grant number GR/M 45764.

A Appendix

This appendix presents key quaternion mathematical relations. The hypercomplex numbers discovered by Hamilton [5] in 1843 are viewed as a generalisation of the complex numbers. A quaternion q is given by:

$$q = w + xi + yj + zk \quad (3)$$

where w , x , y and z are real, and i , j and k are complex operators bound by the following relations:

$$\begin{aligned} ij &= k & jk &= i & ki &= j \\ ji &= -k & kj &= -i & ik &= -j \end{aligned} \quad (4)$$

A prominent feature of the quaternions is their non-commutative property and as a consequence, convolution using quaternions requires both the right and left convolution

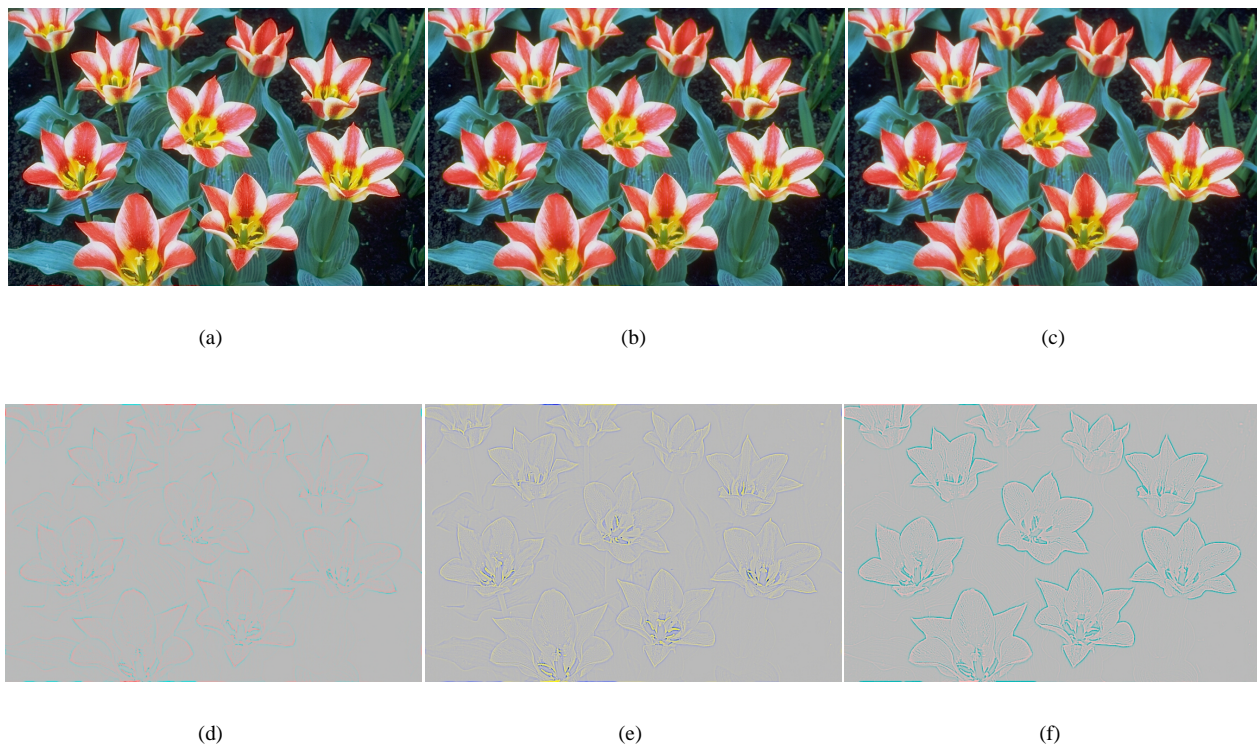


Figure 6: From left to right on the top row the images are filtered in the red, yellow and green colour direction respectively. From left to right on the bottom row are the “difference images” between the original (Figure 5) and respective filtered images in the top row.

mask (one mask on the left and another mask on the right side of the image). Non-commutativity is characteristic of vectors and it is also true for the hypercomplex numbers whose 3 imaginary parts form a vector. In terms of the RGB colour space, x , y and z represent red, green and blue components of a pixel respectively.

The magnitude of the pure quaternion (scalar part is zero) can be used as a measure of the distance between the colour and mid-grey [6]. Mid-grey is located at the origin of the hypercomplex space. Normalising a quaternion representation of a colour discards distance information, but retains the orientation information of the colour relative to mid-grey.

A unit pure quaternion (vector) is obtained from an arbitrary vector by:

$$\mu = \frac{\mathbf{i}x + \mathbf{j}y + \mathbf{k}z}{\sqrt{x^2 + y^2 + z^2}} \quad (5)$$

References

- [1] S. J. Sangwine. Colour image edge detector based on quaternion convolution. *Electronics Letters*, 34(10):969–971, 14 May 1998.
- [2] C. J. Evans, S. J. Sangwine, and T. A. Ell. Colour-sensitive edge detection using hypercomplex filters. In Moncef Gabbouj and Pauli Kuosmanen, editors, *Proceedings of EUSIPCO 2000, Tenth European Signal Processing Conference*, volume I, pages 107–110, Tampere, Finland, 5–8 September 2000. European Association for Signal Processing.
- [3] C. J. Evans, T. A. Ell, and S. J. Sangwine. Hypercomplex color-sensitive smoothing filters. In ICIP2000 [7], pages 541–544.
- [4] T. A. Ell and S. J. Sangwine. Hypercomplex Wiener-Khinchine theorem with application to color image correlation. In ICIP2000 [7], pages 792–795.
- [5] William R. Hamilton. *Elements of Quaternions*. Longmans, Green and Co., London, 1866.
- [6] S. J. Sangwine. Colour in image processing. *Electronics & Communications Engineering Journal*, 12(5):211–219, October 2000.
- [7] *IEEE International Conference on Image Processing (ICIP 2000)*, Vancouver, Canada, 11–14 September 2000. Institute of Electrical and Electronics Engineers.